Imaging properties of the light sword optical element used as a contact lens in a presbyopic eye model

K. Petelczyc,[1] S. Bará,[2] A. Ciro Lopez,[3,4] Z. Jaroszewicz,[5,6] K. Kakarenko[1], A. Kolodziejczyk,[1,*] and M. Sypek[1]

[1]*Faculty of Physics, Warsaw University of Technology, Koszykowa 75, 00-662 Warsaw, Poland*
[2]*Area de Optica, E.U., Optica e Optometria, Universidade de Santiago de Compostela, 15782 Santiago de Compostela, GALIZA, Spain*
[3]*Grupo de Óptica y Fotónica, Instituto de Física, Universidad de Antioquia, A.A1226, Medellín, Colombia*
[4]*Facultad de Ciencias, Instituto Tecnológico Metropolitano, calle 73 #76A-354, Medellín, Colombia*
[5]*Institute of Applied Optics, Kamionkowska 18, 03-805 Warsaw, Poland*
[6]*National Institute of Telecommunications, Szachowa 1, 04-894 Warsaw, Poland*
[*]*kolodz@if.pw.edu.pl*

Abstract: The paper analyzes the imaging properties of the light sword optical element (LSOE) applied as a contact lens to the presbyopic human eye. We performed our studies with a human eye model based on the Gullstrand parameterization. In order to quantify the discussion concerning imaging with extended depth of focus, we introduced quantitative parameters characterizing output images of optotypes obtained in numerical simulations. The quality of the images formed by the LSOE were compared with those created by a presbyopic human eye, reading glasses and a quartic inverse axicon. Then we complemented the numerical results by an experiment where a 3D scene was imaged by means of the refractive LSOE correcting an artificial eye based on the Gullstrand model. According to performed simulations and experiments the LSOE exhibits abilities for presbyopia correction in a wide range of functional vision distances.

OCIS codes: (080.2740) Geometric optical design; (110.2990) Image formation theory; (220.3620) Lens system design; (330.4060) Vision modeling; (330.7323) Visual optics, aging changes.

References and links

1. P. Artal and J. Tabernero, "Optics of human eye: 400 years of exploration from Galileo's time," Appl. Opt. **49**(16), D123–D130 (2010).
2. B. K. Pierscionek, "What we know and understand about presbyopia," Clin. Exp. Optom. **76**(3), 83–90 (1993).
3. A. Glasser, M. A. Croft, and P. L. Kaufman, "Aging of the human crystalline lens and presbyopia," Int. Ophthalmol. Clin. **41**(2), 1–15 (2001).
4. Z. Zalevsky, "Extended depth of focus imaging: a review," SPIE Rev. **1**(1), 018001 (2010).
5. A. Kołodziejczyk, S. Bara, Z. Jaroszewicz, and M. Sypek, "The light sword optical element – a new diffraction structure with extended depth of focus," J. Mod. Opt. **37**(8), 1283–1286 (1990).
6. K. Petelczyc, J. A. García, S. Bará, Z. Jaroszewicz, K. Kakarenko, A. Kolodziejczyk, and M. Sypek, "Strehl ratios characterizing optical elements designed for presbyopia compensation," Opt. Express **19**(9), 8693–8699 (2011).
7. A. Valberg, *Light Vision Color* (Wiley, 2005).
8. H. Gross, F. Blechinger, and B. Achtner, *Handbook of Optical Systems, Vol. 4, Survey of Optical Instruments* (Wiley-VCH, 2008).
9. M. Sypek, "Light propagation in the Fresnel region. New numerical approach," Opt. Commun. **116**(1-3), 43–48 (1995).
10. M. Sypek, C. Prokopowicz, and M. Gorecki, "Image multiplying and high-frequency oscillations effects in the Fresnel region light propagation simulation," Opt. Eng. **42**(11), 3158–3164 (2003).
11. J. Ares García, S. Bará, M. Gomez García, Z. Jaroszewicz, A. Kolodziejczyk, and K. Petelczyc, "Imaging with extended focal depth by means of the refractive light sword optical element," Opt. Express **16**(22), 18371–18378 (2008).
12. J. H. McLeod, "The axicon: a new type of optical element," J. Opt. Soc. Am. **44**(8), 592–597 (1954).

#153517 - $15.00 USD Received 25 Aug 2011; revised 6 Oct 2011; accepted 14 Oct 2011; published 30 Nov 2011

13. Z. Jaroszewicz, *Axicons: Design and Propagation Properties, Research & Development Treaties*, (SPIE Polish Chapter, Warsaw, 1997), Vol. 5.
14. J. Sochacki, A. Kołodziejczyk, Z. Jaroszewicz, and S. Bará, "Nonparaxial design of generalized axicons," Appl. Opt. **31**(25), 5326–5330 (1992).
15. W. Chi and N. George, "Electronic imaging using a logarithmic asphere," Opt. Lett. **26**(12), 875–877 (2001).
16. J. Ares, R. Flores, S. Bará, and Z. Jaroszewicz, "Presbyopia compensation with a quartic axicon," Optom. Vis. Sci. **82**(12), 1071–1078 (2005).
17. G. Mikuła, Z. Jaroszewicz, A. Kolodziejczyk, K. Petelczyc, and M. Sypek, "Imaging with extended focal depth by means of lenses with radial and angular modulation," Opt. Express **15**(15), 9184–9193 (2007).
18. G. Mikuła, A. Kolodziejczyk, M. Makowski, C. Prokopowicz, and M. Sypek, "Diffractive elements for imaging with extended depth of focus," Opt. Eng. **44**, 058001(1–7) (2005).
19. J. W. Goodman, *Introduction to Fourier Optics* (Roberts & Company, 2005).
20. D. Moore, *Basic Practice of Statistics*, (W. H. Freeman and Company, 2010).
21. B. Pan, K. Qian, H. Xie, and A. Asundi, "Two-dimensional digital image correlation for in-plane displacement and strain measurement: a review," Meas. Sci. Technol. **20**, 062001(17pp) (2009).

1. Motivation

At birth the human eye has outstanding abilities to change its optical power by accomodation. During life the accommodation amplitude decreases almost linearly about 0.2D per year. After the age of about 50 years the accommodation usually decreases to less than 1D. This dysfunction is called presbyopia and makes it impossible to accommodate distant and near parts of a spatial scene even with the use of conventional spectacles [1–3]. Therefore substantial efforts have been made to create some correction methods substituting the lack of accommodation by means of imaging with extended depth of focus (EDOF) [4].

This paper continues investigations on application of the light sword element (LSOE) [5] for ophthalmic purposes. As has been shown lately, studies analyzing Strehl ratios lead to the conclusion that the LSOE can be a promising element for presbyopia correction [6]. Nevertheless, the Strehl ratio offers somewhat limited insight into the imaging process. A valuable assessment regarding the usefulness of the LSOE requires a more detailed analysis. Therefore we decided to investigate in detail the quality of imaging realized by the LSOE in a set-up simulating a presbyopic naked eye. The paper presents images of the Snellen E and the Landolt C optotypes of constant angular dimensions equal to 5 arcmin in the retinal space. Numerical simulations were conducted according to those described in Ref. [6]. We assumed a human eye model based on the simplified Gullstrand parameterization [7,8] and then obtained final results of calculations by means of the same software package based on a convolution method [9,10]. For comparison, simulations were performed versus a naked presbyopic eye (EYE) and an EYE corrected with an LSOE contact lens, monofocal reading glasses (RG) and an inverse quartic axicon (IQAX). The Strehl ratios corresponding to these arrangements were analyzed in Ref. [6]. In order to get a more objective assessment of output images quality, we used quantitative criteria of imaging.

Experiments with an artificial presbyopic eye completed our studies. We constructed an arrangement simulating an eye according to the Gullstrand model. A spatial scene was imaged by the setup corresponding to a naked eye and then by the same setup corrected with a refractive LSOE and a refractive monofocal lens simulating reading glasses. Both corrective elements were fabricated by photosculpture in Ormocer™ photoresist using grayscale masks [11].

2. Eye model and compensating elements

In our investigations we assumed the simplified Gullstrand model of the human presbyopic eye discussed in Ref. [6]. We selected this model as relatively simple for numerical modeling and at the same time illustrating the structure of the human eye. According to the Gullstrand parameterization the relaxed human eye consists of the cornea (43 D) and the eye lens (19.2 D) immersed in a liquid with a refractive index equal to 1.336. Both elements can be regarded as thin ones situated at a mutual distance of 5.38mm. The output retinal plane is located 18.76mm behind the eye lens. Figure 1 illustrates a scheme of the model. It determines the reference set-up termed as the EYE enabling acute vision at infinity.

#153517 - $15.00 USD Received 25 Aug 2011; revised 6 Oct 2011; accepted 14 Oct 2011; published 30 Nov 2011

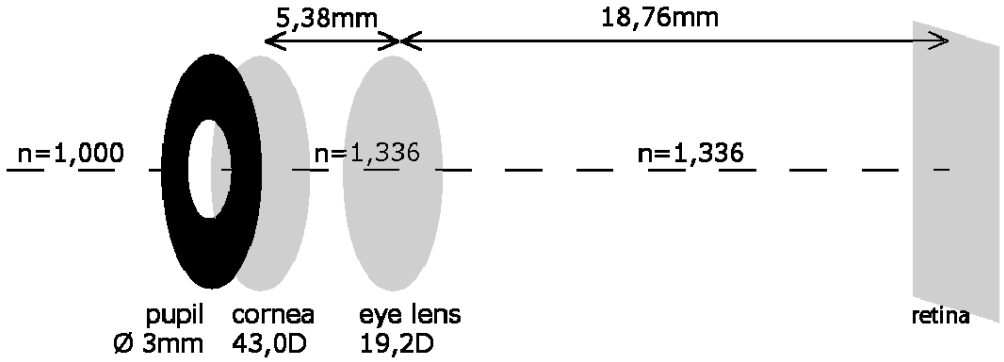

Fig. 1. A scheme of the presbyopic human eye model based on the Gullstrand parameterization.

Moreover during performed simulations we studied the EYE corrected with three different elements forming modified arrangements (RG, IQAX, LSOE). According to our assumptions the following corrective elements were placed just before the cornea lens:

2.1 Reading glasses (RG)

Reading glasses make possible clear vision at a reading distance of 25cm. This method of correction does not significantly change accommodation and depth of field. Then, after its application, only close objects can be sharply visible. Because reading glasses work nearly like monofocal contact lenses we model this method of correction by a single lens with power +4D placed just before the cornea lens. This simplification enables us to analyze reading glasses in the same way like other compensating elements.

2.2 Inverse quartic axicon (IQAX)

Axicons possess radial symmetry and focus light into a focal segment [12,13]. Hence these elements are especially suited for EDOF imaging [14,15]. An axicon is a generalization of the idea of multifocal lenses. Such lenses available in the ophthalmic market have concentric rings with alternate optical power. Axicons reveal optical powers that change continuously with the lateral polar coordinate. According to our former studies Strehl ratios of axicons and multifocal lenses exhibit similar imaging properties [6]. Therefore from elements of this kind we chose the IQAX for more detailed investigations. As was already shown, this element has valuable EDOF imaging properties and can be potentially useful in ophthalmology [16]. The optical path difference (OPD) introduced by the IQAX with the diameter 2R = 3 mm is given as follows:

$$\begin{aligned} &\Delta l(r) = Ar^4, \\ &A = -\frac{Add}{4R^2} \quad \text{for } r \le R, \\ &A = 0 \qquad \text{for } r > R, \end{aligned} \tag{1}$$

where r is the radial coordinate in the polar coordinate system and Add (= 4D) denotes the addition. For a chosen diameter 3mm the axicon fills exactly an iris aperture fulfilling the most suitable condition for photopic vision [6,8].

2.3 Light sword optical element (LSOE)

This corrective element causes an angular modulation of the optical power. The cornea of the presbyopic eye compensated by such structure constitutes a system being equivalent to the LSOE [5] and providing the following OPD:

#153517 - $15.00 USD Received 25 Aug 2011; revised 6 Oct 2011; accepted 14 Oct 2011; published 30 Nov 2011

$$\Delta l(r,\theta) = -\frac{r^2}{2\left(f_1 + \frac{\Delta f \theta}{2\pi}\right)}, \tag{2}$$

where θ is the azimuthal coordinate in the polar coordinate system. Then each infinitesimal angular sector corresponds to a spherical lens with a focal length $f + \Delta f\theta/2\pi$. Therefore the LSOE focuses approximately a plane wave into a focal segment stretched from f up to $f + \Delta f$ behind the structure. A more detailed analysis according to the ray tracing method shows that focusing is not perfect within the geometrical optics [17]. On the other hand numerical and experimental results demonstrate usefulness of the LSOE for EDOF imaging [6,11,17,18].

The last two elements (IQAX, LSOE) compensate EYE shown in Fig. 1 and they are designed in order to cover defocus from 0 D up to +4 D corresponding to the object distances range $[25\text{cm}, +\infty)$.

3. Numerical simulations of imaging

In the numerical simulations we analyzed presbyopic vision without correction (EYE) and with the use of three elements described above (RG, IQAX, LSOE). As the test object we chose a set of optotypes: the Snellen E and the Landolt C being of widespread use in ophthalmology. The idea of optotypes vision tests needs constant angular dimensions, which means that optotypes grow with object distance and stay unchanged in the retinal plane. Details of the used optotypes presented in Fig. 2 have an angular size equal to 1 arcmin in the retinal space. That size corresponds to the standard resolution of normal emmetropic eyes.

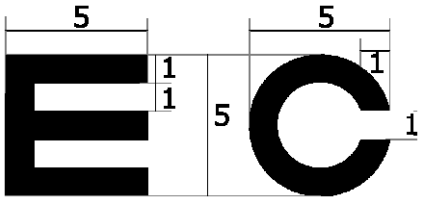

Fig. 2. An ideal image of the Snellen E and the Landolt C obtained in the central fragment of the imaging plane with dimensions 33 μm x 33 μm. Presented units denote the angular size in minutes of arc in the retinal space.

Similarly to our previous work [6] we conducted numerical simulations by means of software based on the modified convolution method [9,10]. We assumed monochromatic, spatially incoherent light with a wavelength 555nm corresponding to the highest sensitivity of the human eye in photopic vision [7,8]. Small dimensions of output images allow us to restrict our investigations to the small foveal region of the retina where vision is the most acute. This assumption makes possible to apply the paraxial approximation and the isoplanarity of the imaging system in calculations of light propagation and during the design of compensating optical elements. The simulations are performed in the set-up presented in Fig. 1. They begin with the creation of a spherical wave divergent from an axial point lying in an object plane. Then the wave amplitude is equalized in the iris plane and multiplied by the phase transmittance of the compensating element, the corneal lens and an amplitude factor being responsible for the Stiles-Crawford effect: $\exp(-0.053r^2)$, where r is expressed in mm [8]. After propagation in a liquid medium the light field is modified by the transmittance of the eye lens and then we perform another propagation to the retinal plane where the output complex amplitude is formed. The square modulus of this amplitude defines the point spread function (PSF). Taking into account the assumed isoplanarity of the system the final irradiance image is defined as the convolution of the PSF with the ideal irradiance distribution shown in Fig. 2 [19]. In order to make our analysis of imaging more objective we introduced the following two quantitative parameters:

#153517 - $15.00 USD Received 25 Aug 2011; revised 6 Oct 2011; accepted 14 Oct 2011; published 30 Nov 2011

$$W = \sqrt{\frac{\iint \left[I(x,y) - I_{id}(x,y) \right]^2 dxdy}{\iint dxdy}}, \tag{3}$$

$$K = \frac{\iint \left\lfloor I(x,y) - I_m \right\rfloor \left\lfloor I_{id}(x,y) - I_{idm} \right\rfloor dxdy}{\sqrt{\iint \left[I(x,y) - I_m \right]^2 dxdy} \sqrt{\iint \left[I_{id}(x,y) - I_{idm} \right]^2 dxdy}}, \tag{4}$$

where I and I_{id} are the irradiance distributions normalized to the maximal value within the output image and the ideal image respectively. I_m and I_{idm} in Eq. (5) are the mean values of the irradiances defined as follows:

$$I_m = \frac{\iint I(x,y)\,dxdy}{\iint dxdy}, \quad I_{idm} = \frac{\iint I_{id}(x,y)\,dxdy}{\iint dxdy}. \tag{5}$$

The calculations were limited to a central region of the retinal plane, in form of a square with dimensions 200 μm × 200 μm. The parameter W is a root mean square deviation which grows with the quality drop of the output images. This value goes to zero in the ideal case of imaging. The parameter K can be regarded as a correlation coefficient [20], [21]. This parameter increases with image quality.

Figure 3-6 present the output images in the retinal plane created by EYE without correction and with compensating elements (RG, IQAX, LSOE) located in the corneal plane. Additionally during simulations we assumed a limited iris aperture diameter equal to 3 mm. This value corresponds to the optimal resolution of photopic vision realized by the foveal region of the human eye [8]. As expected, the presbyopic eye forms sharp images of only far optotypes. The RG reverses the defocus range and allows to observe satisfactorily objects located at a distance of 25cm. Images created by the IQAX and by the LSOE generally confirm results from Ref. [6]. The IQAX, though designed for object distances from 25cm up to infinity, is able to compensate only a moderate defocus. Then acceptable imaging is limited to objects lying beyond 60cm. Images of near optotypes have a poor contrast and remain unrecognizable. Unlike the IQAX, the LSOE forms acceptable images for the whole assumed range of defocus (up to +4 D). The quality of imaging is almost constant for all object distances from 25 cm.

Moreover Fig. 3-6 indicate the values of the parameters W and K. Optotypes recognition depends strongly on the individual perception. Thus it is difficult to give an explicit criterion. Nevertheless, analyzing images shown in Figs. 3-6 one can state that the majority of images are recognizable when the parameters W, K fulfill simultaneously the following inequalities: W<0.2 and K>0.7. Figure 7 presents plots of the quantitative parameters with varying defocus for the Snellen optotype E. Bold lines with dots correspond to the values shown in Fig. 3-6 when the iris diameter is 3mm. Fine lines with crosses represent additional results for a diameter equal to 5mm. Recognition criteria defined by the given inequalities (W<0.2 and K>0.7) are fulfilled by the EYE, the RG and the IQAX in a limited range of defocus. For the smallest iris diameter it is only 0D-0.5D and 3.5D-4D for the EYE and the RG respectively. Larger apertures narrow these ranges even more. The quality parameters of images formed by the IQAX are in the criteria range for a defocus smaller than ca. 2.5 D independently of the aperture diameter (for aperture diameters larger than 3mm the element has an exterior ring with no optical power). Plots describing imaging realized by the LSOE are almost flat and lay properly above or under dashed lines indicating criteria values 0.2 for W and 0.7 for K. It confirms the recognizable character of images in the whole range of assumed defocus. Moreover, since the graphs change only slightly with the aperture diameter, we can suspect similar imaging performance for different iris sizes.

#153517 - $15.00 USD Received 25 Aug 2011; revised 6 Oct 2011; accepted 14 Oct 2011; published 30 Nov 2011

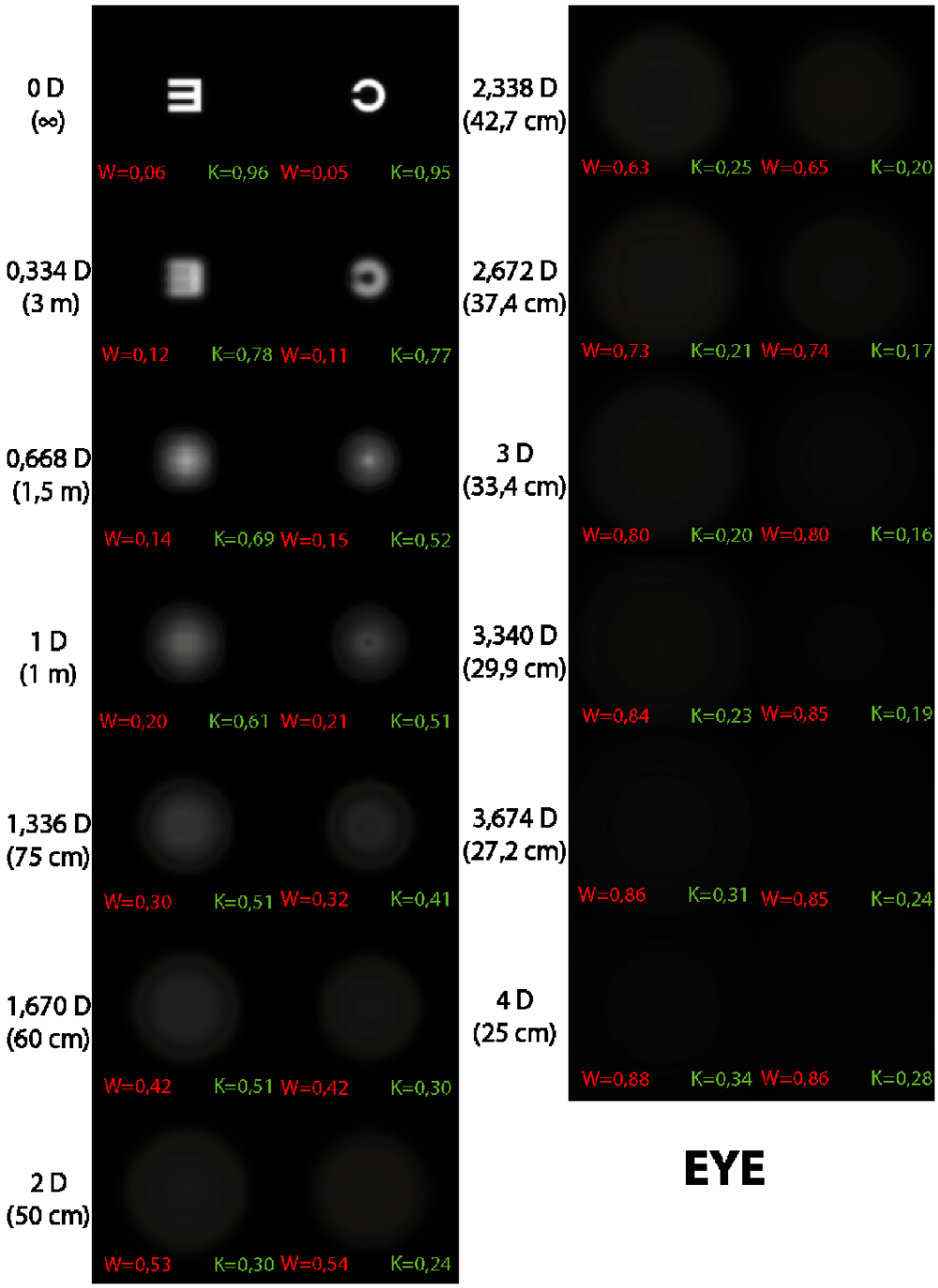

Fig. 3. Images of optotypes formed by the presbyopic eye. Defocus powers and related object distances are given in the left side. Each individual image corresponds to a square retinal region with dimensions 200 μmx200 μm. Other notations are explained in the text.

#153517 - $15.00 USD Received 25 Aug 2011; revised 6 Oct 2011; accepted 14 Oct 2011; published 30 Nov 2011

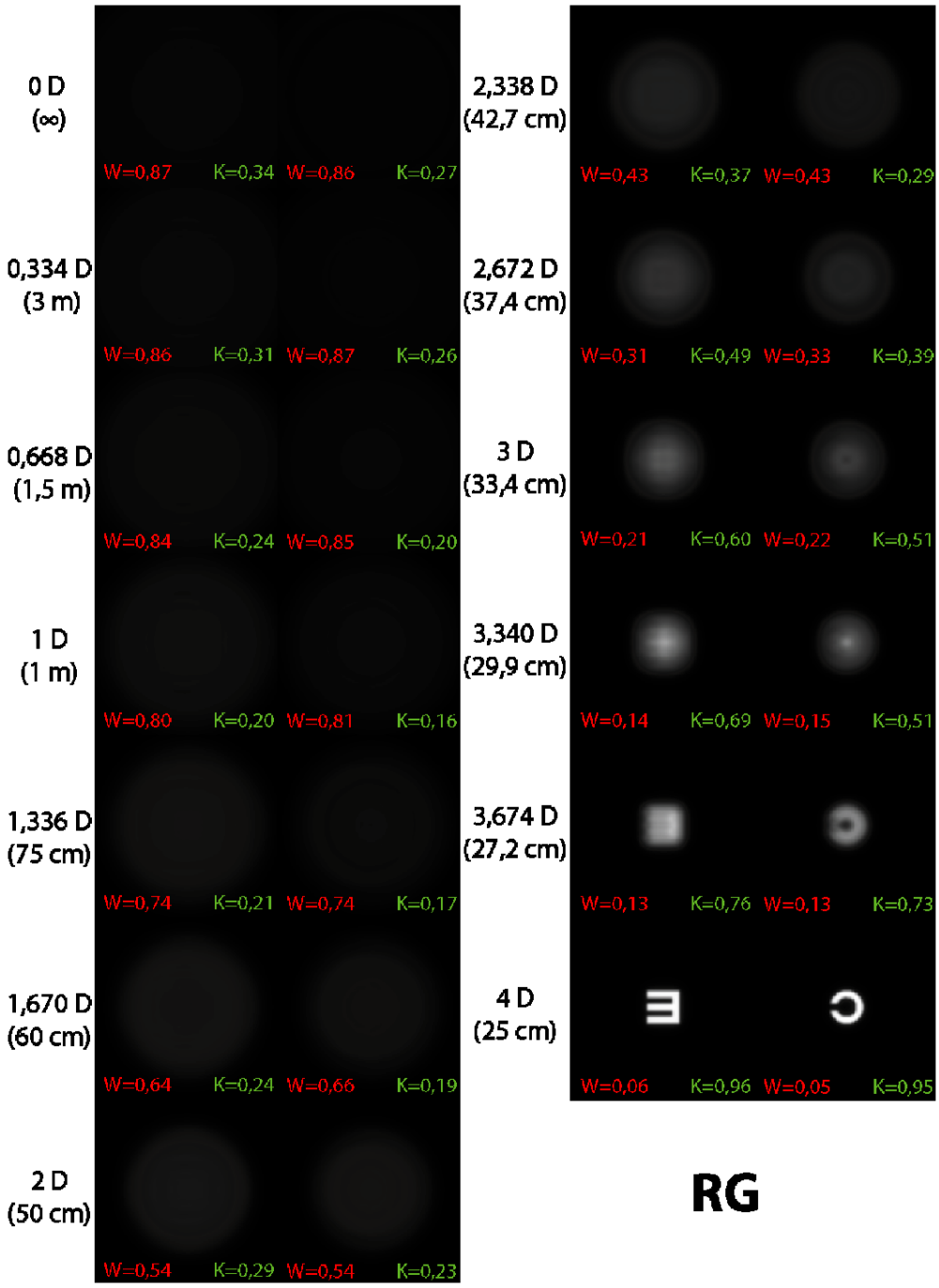

Fig. 4. Images of optotypes formed by the presbyopic eye compensated by reading glasses. Defocus powers and related object distances are given in the left side. Each individual image corresponds to a square retinal region with dimensions 200 μmx200 μm. Other notations are explained in the text.

#153517 - $15.00 USD Received 25 Aug 2011; revised 6 Oct 2011; accepted 14 Oct 2011; published 30 Nov 2011

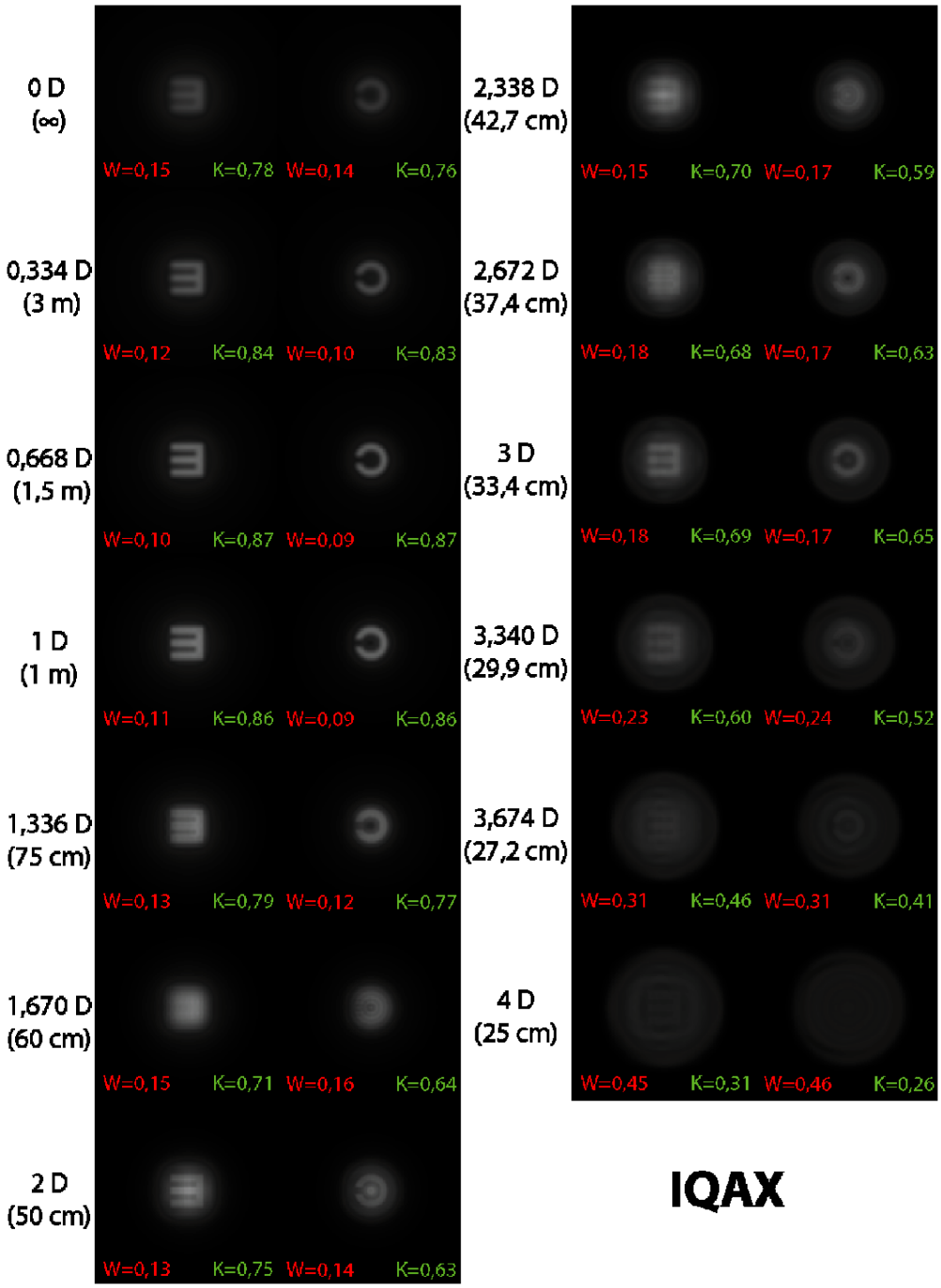

Fig. 5. Images of optotypes formed by the presbyopic eye compensated by an inverse quartic axicon. Defocus powers and related object distances are given in the left side. Each individual image corresponds to a square retinal region with dimensions 200 μmx200 μm. Other notations are explained in the text.

#153517 - $15.00 USD Received 25 Aug 2011; revised 6 Oct 2011; accepted 14 Oct 2011; published 30 Nov 2011

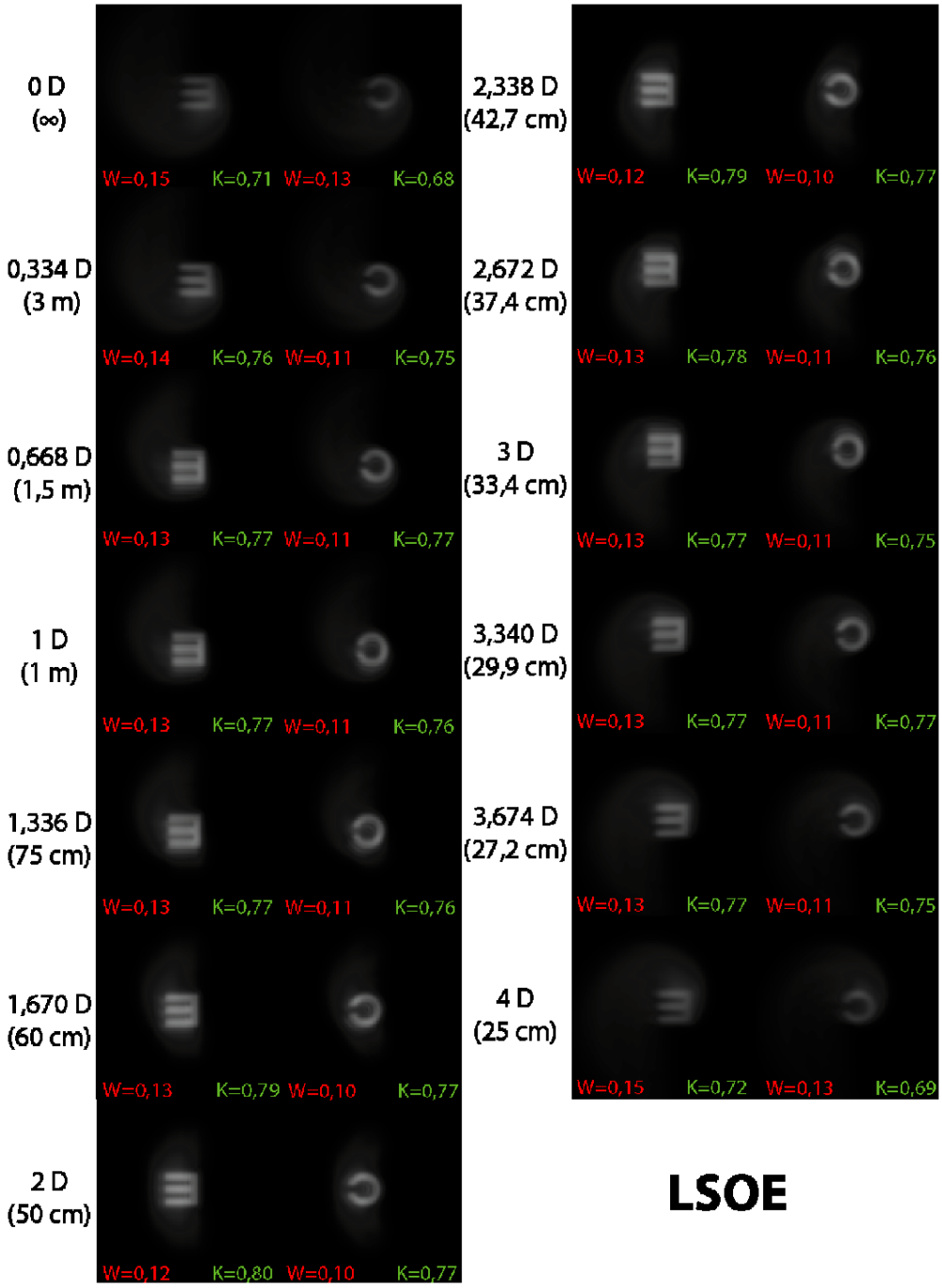

Fig. 6. Images of optotypes formed by the presbyopic eye compensated by a light sword optical element. Defocus powers and related object distances are given in the left side. Each individual image corresponds to a square retinal region with dimensions 200 μmx200 μm. Other notations are explained in the text.

#153517 - $15.00 USD Received 25 Aug 2011; revised 6 Oct 2011; accepted 14 Oct 2011; published 30 Nov 2011

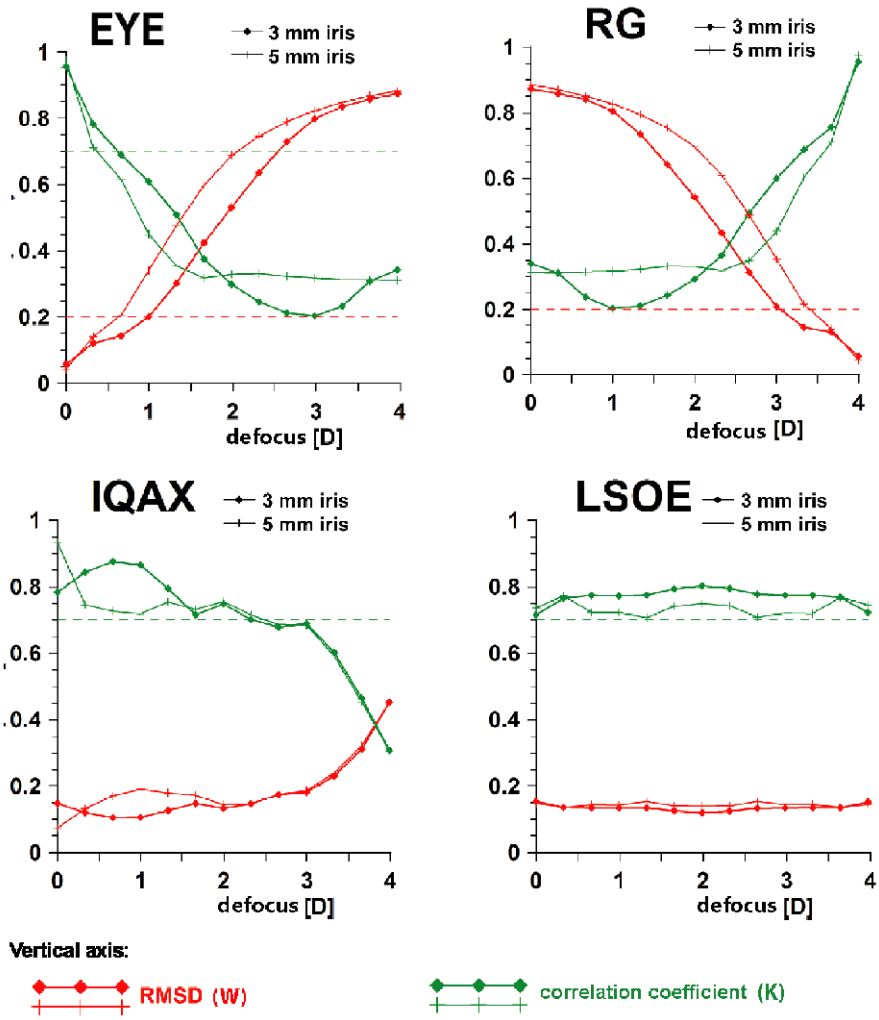

Fig. 7. Quantitative parameters of images of the Snellen E optotype formed by a presbyopic eye without correction (EYE) and after correction with compensating elements (RG, IQAX, LSOE). Results correspond to iris diameters 3mm and 5 mm. Other notations are explained in text.

4. Experiment

Previous findings on the LSOE allow to hope that this element can be useful for presbyopia compensation. Nevertheless, results obtained hitherto in arrangements modeling the human eye have limited significance because they were restricted to numerical simulations or experiments with diffractive elements in monochromatic light [6,17]. In order to complement this deficiency we decided to perform an experiment with an artificial presbyopic eye based on the Gullstrand model consisting of refractive lenses. Using this set-up compensated by the LSOE and the monofocal lens simulating reading glasses we imaged a 3D scene in white light. Compensating elements were fabricated in refractive forms in photoresist according to the same technique.

4.1 The artificial eye

The construction of the artificial eye is based on the simplified Gullstrand model of the human eye [8] illustrated in Fig. 1. The refractive elements should be immersed in a liquid with

#153517 - $15.00 USD Received 25 Aug 2011; revised 6 Oct 2011; accepted 14 Oct 2011; published 30 Nov 2011

refractive index 1.336. Nevertheless, the experiment needs additional modification because the retina modeled in our arrangement by a CCD matrix must work in the air. The liquid's removal violates the asymmetry in the object and the image space resulting in an incorrect image magnification and a different range of the field depth. Because both parameters are very important in the context of our work, we decided to scale the optical powers of the system as well as the object distances and the aperture diameter by a factor 1.336 equal to the refractive index of the liquid. This assumption mainly determines the structure of the artificial eye.

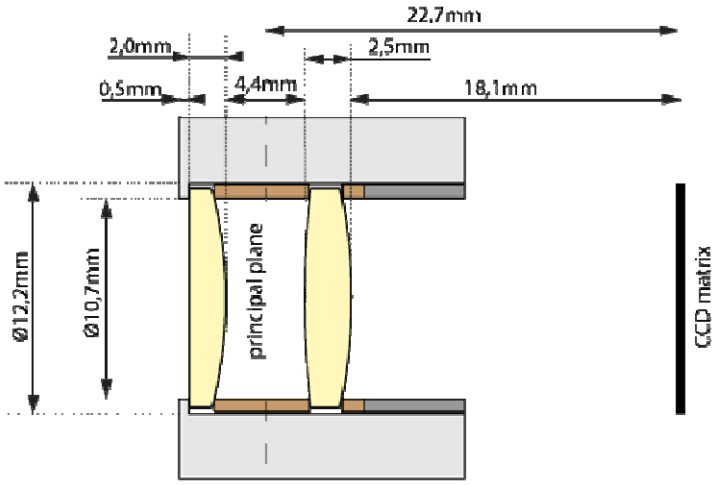

Fig. 8. A scheme of the artificial presbyopic eye with indicated dimensions and distances.

Additionally, in reality we cannot use thin lenses. The compensating elements were fabricated onto flat substrates. In order to ensure good optical contact we modeled the cornea as a plane-convex lens. Manufacturing a second biconvex lens representing a lens of the human eye we preserved the same relation between curvature radii of surfaces as in the Gullstrand model. The lenses were produced in BK 7 glass. The optical power of the corneal model 32 D (43 D/1.336) determines its curvature radius equal to 16.5mm. Similarly, the lower optical power of the second lens 14.4 D (19.2 D/1.336) defines curvatures being equal to 57.45mm and 95.76mm. Finally, the distances between the lenses and the location of the CCD matrix were given by an assumed optical power of the system being 1.336 times smaller in relation to that in the Gullstrand model. Figure 8 presents a detailed scheme of the set-up while the whole constructed arrangement used in an experiment is shown in Fig. 9.

Note, that our assumptions about scaling introduce a difference between the artificial eye and the Gullstrand model. The output images formed by the constructed arrangement and the simplified Gullstrand eye have the same structure but experimental object distances as well as iris diameters are 1.336 times greater.

4.2 Refractive compensating elements

We fabricated a refractive LSOE by photolithography in sol-gel Ormocer^{TM} photoresist deposited onto a 1mm thick glass substrate of 25.4mm diameter. A gray scale mask corresponding to the local thickness of the LSOE was made and then used in a photosculpture process. The fabrication resulted in an element with a diameter of 4.77mm and a maximal thickness of about 25μm. Figure 10 presents the produced refractive LSOE, its interferogram obtained in a Mach-Zehnder interferometer and the bitmap of an ideal interferogram. Manufacturing errors are clearly visible, but the LSOE demonstrates satisfactory EDOF abilities. According to the shown interferogram and experimental results its optical powers correspond roughly to a range [0.33 D, 2 D] covering object distances from 5 cm up to 3m in

#153517 - $15.00 USD Received 25 Aug 2011; revised 6 Oct 2011; accepted 14 Oct 2011; published 30 Nov 2011

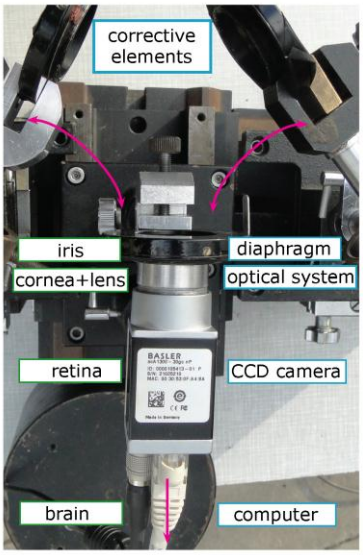

Fig. 9. A photograph of the artificial presbyopic eye. Blue inscriptions denote parts of human eye and black ones indicate corresponding elements in the constructed model.

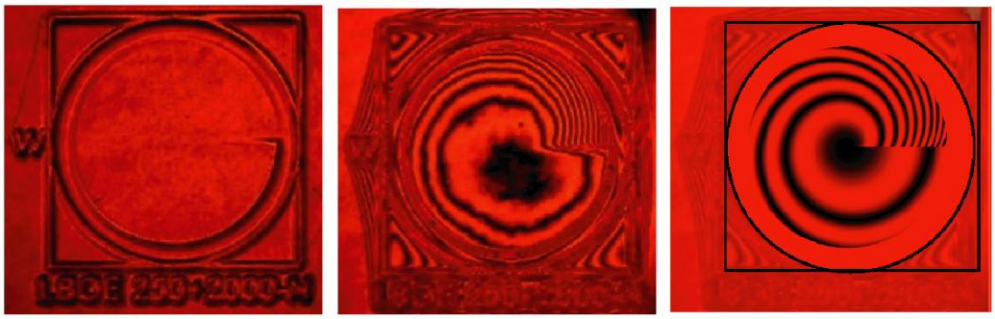

Fig. 10. The refractive LSOE (left) and its interferogram (center) obtained in a Mach-Zehnder interferometer with a use of monochromatic light with λ = 632,8 nm. The right image shows the numerical interferogram of the ideal phase transmittance

our set-up with the artificial eye. For an experimental comparison, the monofocal lens simulating reading glasses was produced with the same technique. The obtained element has an optical power equal to about 3.8 D. Imperfections of fabrication similar to the former case stretched substantially a focal range of the lens, which leads to expected object distances from 22cm up to 28cm.

4.3 Experimental results

Using the constructed model and the fabricated refractive structures we imaged a 3D scene consisting of scrabble bricks, boxes and toys. All elements were located at different distances and illuminated by bulb lamps. The average illuminance was equal to 500 lx. Figure 11 shows the sketch of the spatial arrangement with marked distances and dimensions. The scene was registered by the artificial eye alone and with compensation by means of the refractive LSOE and the refractive monofocal lens. These three cases correspond to EYE, RG and LSOE in the presented numerical simulations. The compensating elements simulating contact lenses were fixed to the plane side of the lens representing the cornea. Figures 12-14 (Media 1, Media 2, Media 3) present images recorded by the CCD matrix of the artificial eye. Images shown in

#153517 - $15.00 USD Received 25 Aug 2011; revised 6 Oct 2011; accepted 14 Oct 2011; published 30 Nov 2011

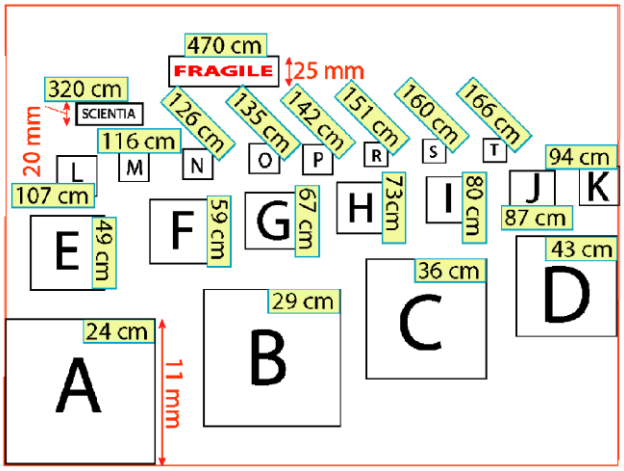

Fig. 11. Arrangement of the 3 D scene used in the experiment. Black numbers denote object distances and orange numbers indicate dimensions of particular elements. All letter bricks have in reality the same size.

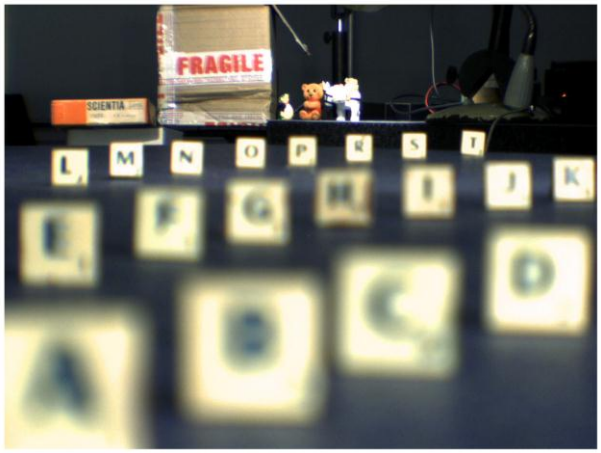

Fig. 12. The 3 D scene imaged by the artificial eye (Media 1).

Figs. 12, 13 (Media 1, Media 2) were taken under identical settings and they coincide well with the numerical simulations. Only distant or near objects are satisfactorily registered. The depth of field of the monofocal lens seems to be stretched because of manufacturing imperfections so three closest brick are well visible. According to Fig. 14 (Media 3) the LSOE can expressly compensate defocus realized by the constructed eye. In spite of substantial aberrations of the element caused by the fabrication process all scene's fragments related to object distances from 50cm to 3m are recognizable. What is extremely important is that the refractive LSOE does not exhibit chromatic aberrations. With respect to this inconvenience images formed without compensation (Fig. 12 (Media 1)) and with compensation by the LSOE (Fig. 14 (Media 3)) do not show noticeable differences.

#153517 - $15.00 USD Received 25 Aug 2011; revised 6 Oct 2011; accepted 14 Oct 2011; published 30 Nov 2011

Fig. 13. The 3 D scene imaged by the artificial eye compensated by the monofocal lens (Media 2).

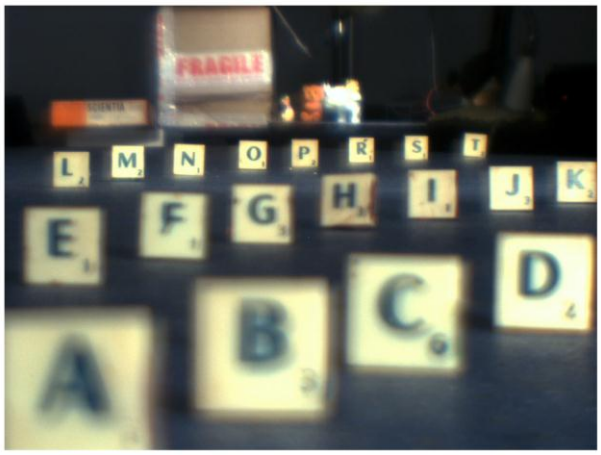

Fig. 14. The 3 D scene imaged by the artificial eye compensated by the LSOE (Media 3).

5. Conclusions

In this work the usefulness of the LSOE for presbyopia correction was analyzed. The investigations were conducted using a model of the presbyopic human eye based on the Gullstrand parameterization. We performed numerical simulations of optotypes imaging for the presbyopic eye, the monofocal lens simulating reading glasses, the LSOE, and an inverse quartic axicon representing here elements of radial symmetry as axicons and multifocal lenses designed especially for EDOF imaging. According to the obtained results the LSOE -unlike other elements - can correct defocus in the assumed range from 0 D to 4 D covering all functional vision distances. What is important, the quality of the images formed by the LSOE is almost independent on the iris diameter (Fig. 7). This conclusion coincides well with the element's geometry. All angular sectors of the LSOE responsible for different focal lengths (or optical powers) take part in the imaging process for any arbitrary aperture size. For ophthalmic purposes it can be a valuable advantage over elements with radial symmetry where an aperture's change substantially affects the range of defocus compensation.

The human eye usually operates in white light. Therefore we decided to perform the experiment with such illumination. For this purpose we constructed a model of the presbyopic human eye based on the Gullstrand parameterization. During an imaging experiment

#153517 - $15.00 USD Received 25 Aug 2011; revised 6 Oct 2011; accepted 14 Oct 2011; published 30 Nov 2011

defocusing caused by the artificial eye was compensated by the refractive LSOE and the refractive monofocal lens fabricated in a photoresist according to the same technique. Unfortunately, because of manufacturing imperfections the produced LSOE revealed substantial aberrations and it covered only partly the assumed range of focal distances. In spite of this disadvantage the refractive LSOE exhibits distinct abilities for EDOF imaging. Both distant and near elements of the scene are recognizable (Fig. 14 (Media 3)). The acceptable quality of imaging even exceeds the expected range of object distances from 50cm up to 3m. Moreover the experimental image is not noticeably affected by chromatic aberrations which may be especially important for potential ophthalmic applications.

The presented numerical simulations and experiments show that the LSOE seems to be a very promising tool for presbyopia compensation as a contact lens or probably also as an intraocular lens. Nevertheless, one should take into account some disadvantages of this element. The applied angular modulation induces an off-axis shift of the focal line of the LSOE. Focal spots wave slightly around the optical axis and have characteristic tails [17,18,21]. Then the LSOE forms images affected by blurring and weak "ghosts". Fortunately this effect is not very distinct and is hardly visible in Fig. 14 (Media 3). One can hope that this inconvenience can be compensated by the brain image processing procedures and that psychophysical adaptability of the human visual system for the LSOEs aberrations is possible. These important problems are out of scope of this paper and they need further studies and clinical tests.

Acknowledgments

This work was supported by the Polish Ministry of Science and Higher Education under grant N N 514 149038 and by the Spanish Ministerio de Ciencia e Innovación (MICINN), grant FIS2008-03884 with complementary support from the European Social Fund implemented under the Human Capital Programme (POKL), project, "Preparation and Realization of Medical Physics Specialty." A. Ciro López wants to give his thanks to Instituto Tecnologico Metropolitano de Medellin for valuable support and facilitating the necessary labor time for participation in this work.

#153517 - $15.00 USD Received 25 Aug 2011; revised 6 Oct 2011; accepted 14 Oct 2011; published 30 Nov 2011